THE JOURNAL OF BIOLOGICAL CHEMISTRY
Vol. 277, No. 40, Issue of October 4, pp. 36978–36986, 2002
Printed in U.S.A.


# Cloning, Expression, and Functional Characterization of a $Ca^{2+}$-dependent Endoplasmic Reticulum Nucleoside Diphosphatase*

Received for publication, February 19, 2002, and in revised form, July 9, 2002
Published, JBC Papers in Press, August 8, 2002, DOI 10.1074/jbc.M201656200

**Bernd U. Failer, Norbert Braun, and Herbert Zimmermann‡**

*From the Arbeitskreis Neurochemie, Biozentrum der J. W. Goethe-Universitaet, Marie-Curie-Strasse 9, D-60439 Frankfurt am Main, Germany*

**We have isolated and characterized the cDNA encoding a $Ca^{2+}$-dependent nucleoside diphosphatase (EC 3.6.1.6) related to two secreted ATP- and ADP-hydrolyzing apyrases of the bloodsucking insects, *Cimex lectularius* and *Phlebotomus papatasi*. The rat brain-derived cDNA has an open reading frame of 1209 bp encoding a protein of 403 amino acids and a calculated molecular mass of 45.7 kDa. The mRNA was expressed in all tissues investigated, revealing two major transcripts with varying preponderance. The immunohistochemical analysis of the Myc-His-tagged enzyme expressed in Chinese hamster ovary cells revealed its association with the endoplasmic reticulum and also with pre-Golgi intermediates. $Ca^{2+}$-dependent nucleoside diphosphatase is a membrane protein with its catalytic site facing the organelle lumen. It hydrolyzes nucleoside 5′-diphosphates in the order UDP >GDP = IDP >>>CDP but not ADP. Nucleoside 5′-triphosphates were hydrolyzed to a minor extent, and no hydrolysis of nucleoside 5′-monophosphates was observed. The enzyme was strongly activated by $Ca^{2+}$, insensitive to $Mg^{2+}$, and had a $K_m$ for UDP of 216 $\mu$M. $Ca^{2+}$-dependent nucleoside diphosphatase may support glycosylation reactions related to quality control in the endoplasmic reticulum.**

Recently, novel enzyme families have been characterized with the ability to hydrolyze nucleoside triphosphates and/or nucleoside diphosphates. These enzymes have in common a biosynthetic pathway involving the endoplasmic reticulum but differ regarding their cellular location. Their catalytic sites are directed either to the lumen of the endomembrane system or the cell surface, or they are released from cells. This implies that they can either be involved in intraorganellar metabolic reactions or serve extracellular nucleotide metabolism.

The seven members of the ecto-nucleoside triphosphate diphosphohydrolase (E-NTPDase)[1] family hydrolyze nucleoside triphosphates and diphosphates, albeit with varying preference (review and nomenclature in Refs. 1 and 2). All of them have a wide tissue distribution. NTPDase1 to NTPDase3 (CD39, CD39L1, CD39L3) are typical ecto-enzymes and are thought to play a major role in controlling intercellular signaling mediated by nucleoside tri- and diphosphates, including platelet aggregation (3) and synaptic transmission (4). The other four members of this enzyme family have a predominant intracellular localization. The two closely related variants of NTPDase4 (UDPase/hLALPv and hLALP70) are enriched in the Golgi apparatus (UDPase) (5) and in lysosomal/autophagic vacuoles (hLALP70) (6, 7), respectively. Both enzymes hydrolyze a variety of nucleoside tri- and diphosphates but ATP only to a minor extent. The murine orthologue of NTPDase5 was allocated to the ER (ER-UDPase, 8). However, expression of human NTPDase5 (CD39L4) in COS-7 cells resulted in a secreted and soluble form of the enzyme (9), suggesting that it predominates in the ER and can in addition be released into the extracellular space. NTPDase6 (CD39L2) has been allocated to the Golgi apparatus. This nucleotidase is also associated with the cell surface and becomes secreted from transfected cells (10–13). Both enzymes preferentially hydrolyze a variety of nucleoside diphosphates. In addition, NTPDase7 (LALP1) reveals an intracellular (vesicular) distribution and hydrolyzes a variety of nucleoside tri- and diphosphates (14). At present little is known concerning the functional role of the organelle-associated nucleotidases. Based on work with two related and Golgi-located yeast enzymes, GDPase and Ynd1/Apy1p (15–18), it has been suggested that the ER- and Golgi-located mammalian species are involved in protein glycosylation reactions (5, 8, 10).

An additional family of ATP- and ADP-hydrolyzing enzymes (apyrases, EC 3.6.1.5) has been identified in bloodsucking arthropods. The bed bug, *Cimex lectularius* (19), and the sand fly, *Phlebotomus papatasi* (20), secrete a $Ca^{2+}$-dependent apyrase from their salivary glands that facilitates hematophagy by reducing the ADP-induced aggregation of host platelets. Heterologous transfection of the *C. lectularius* apyrase in COS-7 cells resulted in the secretion of a $Ca^{2+}$-dependent apyrase (19). Sequences related to the insect salivary apyrases can be found in mammalian species (19, 20). It therefore appeared possible that these encode secreted apyrases.

We have cloned and sequenced the rat homologue of the soluble *Cimex* apyrase and studied its cellular distribution and catalytic properties. Our results demonstrate that both the cellular localization and the catalytic properties of the mammalian enzyme differ from its insect relatives. It represents a membrane-bound $Ca^{2+}$-dependent nucleoside diphosphatase ($Ca^{2+}$-NDPase) that is targeted to the ER following heterologous expression.

* This work was supported by grants from the Deutsche Forschungsgemeinschaft (SFB 269, A4) and the Fonds der Chemischen Industrie. The costs of publication of this article were defrayed in part by the payment of page charges. This article must therefore be hereby marked "*advertisement*" in accordance with 18 U.S.C. Section 1734 solely to indicate this fact.

*The nucleotide sequence(s) reported in this paper has been submitted to the DDBJ/GenBank™/EBI Data Bank with accession number(s) AJ 312208 and AJ 312207.*

‡ To whom correspondence should be addressed. Tel.: 49-69-798-29602; Fax: 49-69-798-29606; E-mail: h.zimmermann@zoology.uni-frankfurt.de.

[1] The abbreviations used are: E-NTPDase, ecto-nucleoside triphosphate diphosphohydrolase; CHO, Chinese hamster ovary; ER, endoplasmic reticulum; CY3, indocarbocyanin-3; EST, expressed sequence tag; NDPase, nucleoside diphosphatase; TM, transmembrane domain; WGA, wheat germ agglutinin.

## EXPERIMENTAL PROCEDURES

*Material*—SuperScriptII™ human brain pCMV-SPORT 1 cDNA library, SuperScriptII™ rat brain pCMV-SPORT 2 cDNA library, Trizol™ reagent, reverse transcriptase SuperScript™II, cell culture media Ham's F-12 and Dulbecco's modified Eagle's medium, fetal calf serum, horse serum, penicillin, and streptomycin were from Invitrogen. Cloning vector pcDNA3.1(−)/Myc-His B and oligo(dT) cellulose were purchased from Invitrogen. Hybond N membrane, [α-$^{32}$P]dCTP, and the enhanced chemiluminescence system were from Amersham Biosciences. Anti-digoxigenin alkaline phosphatase-conjugated antibody and a chemiluminescent substrate, (disodium 3-(4-methoxyspiro-{1,2-dioxoethane-2′,3-(5′-chloro)tricyclo[3.3.1.1$^{3,7}$]decan}-4-yl)phenyl phosphate), were obtained from Roche Molecular Biochemicals. Sawady *Pwo* DNA polymerase was from Peqlab, Biotechnologie GmbH (Erlangen, Germany). *Taq* DNA polymerase and restriction endonucleases were purchased from MBI Fermentas (St. Leon-Rot, Germany). Nucleoside triphosphate, diphosphate, and monophosphate sodium salts, poly-(D-lysine), phenylmethanesulfonyl fluoride, and proteinase K were obtained from Sigma. Triton X-100 and Triton X-114 were from Serva (Heidelberg, Germany). AlexaFluor-488™-conjugated lectin WGA was from Molecular Probes (Leiden, Netherlands). Rabbit anti-calnexin carboxyl terminus polyclonal antibody was purchased from StressGen (Victoria, B.C., Canada), and the mouse monoclonal antibody against the Myc epitope was derived from clone 9E10. The polyclonal CY3-labeled anti-rabbit IgG, fluorescein isothiocyanate, CY3-labeled anti-mouse IgG antibodies, and horseradish peroxidase-conjugated anti-rabbit secondary antibodies were obtained from Dianova (Hamburg, Germany). The Nucleobond X-500 plasmid purification kit was purchased from Macherey and Nagel (Düren, Germany). Nitrocellulose membranes were from Schleicher & Schüll (Dassel, Germany). The protease inhibitors chymostatin, pepstatin, benzamidine, antipain, and leupeptin were obtained from Calbiochem.

*cDNA Library Screening*—Electrocompetent *Escherichia coli* XL10 gold were transformed with a human brain pCMV-SPORT 1 cDNA library. Approximately $0.5 \times 10^6$ colonies were plated on Luria-Bertani/ampicillin agar plates. A 300-bp PCR fragment (forward primer, 5′-TACCAGATCGAAGGCAGCAA-3′, and reverse primer, 5′-GCAGGCAGACTCATGGATGA-3′; template human brain pCMV-SPORT 1 cDNA library) was labeled with [α-$^{32}$P]dCTP by PCR. Transformants were screened by colony hybridization with the radiolabeled probe. Positive signal areas were amplified and rescreened for single positive colonies.

*Amplification of cDNA and DNA Methods*—The complete coding sequence of the rat $Ca^{2+}$-NDPase was obtained by PCR using the forward primer, 5′-CCATACAGGTCCTGTCCAGAGTGC-3′, the reverse primer, 5′-GGTTTTTATGAGTCCTGGTGTAACACAGC-3′, and a rat brain pCMV-SPORT 2 cDNA library as a template. The resulting 1.3-kb fragment was digested with *Xba*I and cloned into the *Sma*I and *Xba*I restriction sites of the pCMV SPORT 1 vector. An expression vector containing a carboxyl-terminal Myc-tagged sequence was generated by digestion of pCMV SPORT 1/$Ca^{2+}$-NDPase with *Eco*RI, followed by ligation with pcDNA3.1(−)/Myc-His B. 5′-Truncated *myc*-tagged and non-tagged plasmids were obtained by amplification of a 1.2-kb fragment using the forward primer, 5′-TGAATTCCAGTGCTGGCATCCATGACC-3′, the reverse primer, 5′-TAATACGACTCACTATAGGG-3′, and pCMV SPORT 1/$Ca^{2+}$-NDPase as a template. The PCR fragment was digested with *Eco*RI and ligated with *Eco*RI cut pCMV SPORT 1/$Ca^{2+}$-NDPase and pcDNA3.1(−)/Myc-His B.

*cDNA Sequencing and Computational Sequence Analysis*—DNA sequencing was performed by Scientific Research and Development GmbH (Oberursel, Germany). The Omiga 2.0 sequence analysis program (Oxford Molecular Ltd., Oxford, UK) was used for assembling sequencing fragments, translating DNA into amino acid sequences, generating hydrophobicity plots (21), and amino acid sequence alignment (CLUSTAL W algorithm), including establishing the dendrogram. For prediction of transmembrane domains, the software TMpred (www.ch.embnet.org/software/TMPRED form.html) was employed. For signal peptide and sorting analysis, SignalP 2.0 (www.cbs.dtu.dk/services/SignalP-2.0/) and PSORT II (psort.nibb.ac.jp/form2.html) were used. The DNA and deduced amino acid sequences were analyzed for similarity to known sequences with the NCBI Blast Network service (www.ncbi.nlm.nih.gov/BLAST/). Protein motif search was performed using the PROSITE data base (pbil.ibcp.fr/cgi-bin/npsa_automat.pl?page = npsa_prosite.html).

*Expression of Recombinant Proteins*—Chinese hamster ovary (CHO) cells were cultured as previously described (22). Cells were transfected by electroporation with one of the above described plasmids in electroporation buffer (137 mM NaCl, 5 mM KCl, 0.7 mM $Na_2HPO_4$, 6 mM dextrose, 20 mM Hepes at pH 7) using a BTX Electrocell manipulator 600. In control experiments cells were transfected with empty vector alone.

*Preparation of Membrane Fractions*—24 h after electroporation the culture medium of CHO cells was exchanged to remove dead cells and debris. After an additional 10 h, sodium butyrate was added at a final concentration of 6 mM. The conditioned culture medium was removed 48 h after electroporation, and cells were washed twice with phosphate-buffered saline, trypsinized, washed twice in isotonic buffer A (140 mM NaCl, 5 mM KCl, 5 mM $CaCl_2$, 2 mM $MgCl_2$, 10 mM glucose, 10 mM Hepes, pH 7.4), and finally centrifuged at $300 \times g_{av}$. Following resuspension with buffer A, cells were supplemented with protease inhibitors (2 μg/ml chymostatin, 1 μg/ml pepstatin, 1 mM benzamidine, 2 μg/ml antipain, and 2 μg/ml leupeptin), homogenized, and centrifuged for 10 min at $300 \times g_{av}$ at 4 °C. The resulting supernatant was centrifuged at $100{,}000 \times g_{av}$ for 45 min at 4 °C, and pellets were resuspended in 50% glycerol and stored at −20 °C.

*Measurement of Nucleotidase Activities*—Substrate specificity was determined by incubating membrane fractions in phosphate-free solution containing 0.02% Triton X-100, 50 mM Hepes (pH 7.0), 1 mM $CaCl_2$, and 0.5 mM substrate. Samples were heat-inactivated for 4 min at 95 °C prior to determination of inorganic phosphate (23). The optimal pH range was determined using a combined buffer (50 mM Hepes and 50 mM glycine) ranging from pH 6.0 to 10.5, containing 1 mM $CaCl_2$ and 0.5 mM UDP. Metal ion dependence was measured in 50 mM Hepes (pH 7.0), containing 0.5 mM UDP and either $CaCl_2$ or $MgCl_2$ (up to 4 mM). The $K_m$ value for UDP was determined in 50 mM Hepes (pH 7.0) and a substrate/$Ca^{2+}$ ratio of 1:2. Catalytic activity of membrane fractions derived from cells transfected with the empty plasmid was subtracted from that obtained with cDNA-transfected cells.

*Triton X-114 Partitioning*—Membrane fractions corresponding to $0.4 \times 10^6$ cells transfected with full-length or truncated cDNA or with the empty plasmid were diluted in 300 μl of double distilled water, adjusted to 1% Triton X-114, and incubated on ice for 10 min. Aliquots (50 μl) were removed as controls. The remaining solution was incubated at 30 °C for 10 min. After centrifugation ($12{,}000 \times g_{av}$, 25 °C, 5 min) the aqueous phase (detergent-depleted) was removed, and the hydrophobic phase (detergent-enriched) was resuspended in ice-cold buffer (50 mM Hepes, pH 7.0). Total, aqueous, and hydrophobic phases were analyzed for UDPase activity (50 mM Hepes, pH 7.0, 0.5 mM UDP, 1 mM $CaCl_2$, 0.1% Triton X-100).

*Proteinase K Digestion*—Membrane fractions corresponding to 7,750 cells transfected with full-length cDNA or with the empty plasmid were incubated for 30 min at 37 °C in 0.5 mM $CaCl_2$, 25 mM Hepes (pH 7.4) containing either proteinase K (2.5 μg) or Triton X-100 (0.02%), proteinase K (2.5 μg) plus Triton X-100 (0.02%), or vehicle. Proteinase K activity was stopped with phenylmethylsulfonyl fluoride at a final concentration of 1 mM. Enzyme activity was measured in 25 mM Hepes (pH 7.4) containing 0.5 mM UDP, 1 mM $CaCl_2$ in the presence or absence of 0.02% Triton X-100. No Triton X-100 was added during the enzyme assay when the effect of proteinase K alone on nucleotidase activity was to be determined. Inorganic phosphate was determined as described above.

*Immunoblotting*—For Western blot analysis, aliquots of membrane fraction were treated with dithiothreitol and electrophoresed on 15% SDS-polyacrylamide gels. After electrophoresis, proteins were transferred onto nitrocellulose membranes. Immunodetection was performed with the anti-Myc antibody and horseradish peroxidase-conjugated anti-rabbit secondary antibody using the enhanced chemiluminescence method according to the manufacturer's instructions.

*Immunofluorescence Staining*—24 h after transfection, CHO cells ($4 \times 10^4$) were seeded on poly(D-lysine)-coated (10 μg/ml) glasscover slips (10 mm diameter) and cultured for an additional 24 h. Sodium butyrate (6 mM) was added 14 h before analyzing cells. Immunofluorescence was performed either with cells fixed in methanol to analyze the intracellular distribution of antigens or with viable cells to analyze a potential surface location of the antigen (24). A monoclonal anti-Myc antibody (5 μg/ml), a rabbit anti-calnexin polyclonal antibody (diluted 1:200), or AlexaFluor-488™-conjugated wheat germ agglutinin (WGA) (diluted 1:700) was applied. After application of the secondary antibody (anti-rabbit-CY3, anti-mouse-CY3, anti-mouse-fluorescein isothiocyanate), cells were mounted and investigated with an epifluorescence microscope equipped with a MCID 4 imaging analysis system (Imaging Research, St. Catharines, Ontario, Canada) or a confocal laser scanning microscope (Leica, Bensheim, Germany).

*Northern Blot Analysis*—Wistar rats (200–250 g) were obtained from Charles River Wiga (Sulzfeld, Germany). Total RNA from rat intestine, spleen, thymus, lung, skeletal muscle, heart, kidney, liver, and brain were isolated with Trizol™ reagent. Northern blot analysis with poly-

adenylated RNA was performed as previously described (22). The *Acc*65I-digested clone, pCMV Sport 1/$Ca^{2+}$-NDPase, was used as a template for the cRNA probe. The SP6/T7 polymerase and transcription kit from Roche was used to synthesize digoxigenin-labeled single-stranded antisense cRNA probes in accordance with the supplier's instructions.

## RESULTS

*Screening of a Human Brain cDNA Library*—The *C. lectularius* apyrase (accession number AAD09177) was used as query for similarity searches in expressed sequence tag (EST) databases. A 0.9-kb consensus sequence was generated from human ESTs (GenBank™ accession numbers AA337541, BE410063, BE301945, AW409804, and AW402618) and used for primer design. A 300-bp PCR fragment was amplified using forward primer, 5′-TACCAGATCGAAGGCAGCAA-3′, reverse primer, 5′-GCAGGCAGACTCATGGATGA-3′, and the human brain pCMV-SPORT 1 cDNA library as a template. The fragment was radiolabeled and used for library screening. The resulting clone contained a 786-bp coding sequence and a large 3′-untranslated region. The DNA sequence was used for similarity search in human genome databases, leading to sequence completion and chromosomal localization. The gene was located twice as a triple exon variant on chromosome 17 (17q25, accession number NT010664) and on chromosome 3 (accession number AC079359).

*Amplification and Characterization of the Rat cDNA Clone*—The putative human amino acid sequence was used for similarity search in a mouse EST data base. The EST sequences (GenBank™ accession numbers BF582504, AI645519, and the later released mouse mRNA sequence AK006565, which contains an additional 111 bp in the coding sequence) were used for primer design (forward primer, 5′-CCATACAGGTCCTGTCCAGAGTGC-3′, and reverse primer, 5′-GGTTTTTATGAGTCCTGGTGTAACACAGC-3′). A 1.3-kb PCR fragment amplified from the rat brain pCMV SPORT 2 cDNA library revealed an open reading frame of 1209 bp, encoding 403 amino acid residues. The deduced amino acid sequence (Fig. 1*A*) contains one putative *N*-glycosylation site ($Asn^{90}$) and one cysteine residue ($Cys^{289}$). In addition, consensus sites for two cAMP- and cGMP-dependent protein kinase phosphorylation sites, six protein kinase C phosphorylation sites, six casein kinase II phosphorylation sites, and two *N*-myristoylation sites could be identified. We identified an amino-terminal R*X*R*X*R motif between amino acid position 38 and 42 that may function as a ER retention/retrieval motif (25). The calculated molecular mass of the encoded protein is 45.7 kDa with an isoelectric point of 6.2. The hydrophobicity analysis predicts two hydrophobic stretches in the polypeptide chain (Fig. 1*B*), between residues 15 and 35 (weak) and between 45 and 63 (strong), respectively. The prediction of transmembrane domains (TM) generates two alternative models. The strongly preferred model is amino terminus outside, first TM orientation outside to inside, second TM orientation inside to outside, and carboxyl terminus outside (Fig. 1*C*). The second model predicts only one transmembrane domain at the strongly hydrophobic domain (45–63) with the amino terminus inside, the TM orientation inside to outside, and carboxyl terminus outside (Fig. 1*D*). There are three putative start codons in-frame before the second TM. The second start codon is part of the first TM ($Met^{15}$), whereas the third is situated 10 residues upstream the second TM. Signal peptide analysis predicted a signal anchor (probability 0.990) for a sequence starting with the first ATG and a signal peptide (probability 0.656) for a sequence beginning with the third start codon in-frame. A maximum cleavage site probability of 0.495 was predicted at residue 40 of the sequence beginning with the third start codon. For this reason a second and truncated clone was produced by PCR amplification of a 1.2-kb fragment, beginning with the third start codon encoding 373 amino acid residues.

*Relation to Other Sequences*—A mouse homologue of the cloned rat sequence could be located on chromosome 11. An analysis of mouse AK006565, BC020003, and the EST sequences revealed a potential splice variant. The sequence in AK006565 contains a 37-amino acid residue insert at position 213, as compared with the sequence in BC020003 that is homologous to the cloned rat sequence. To investigate the possible existence of a corresponding splice variant in the rat cDNA library, primers were designed around the putative insert site. PCR analysis revealed no indication of a splice variant corresponding to the mouse AK006565 sequence (data not shown).

The deduced amino acid sequence of rat full-length $Ca^{2+}$-NDPase cDNA shares 86 and 95% amino acid identity with the corresponding human and mouse sequences. $Ca^{2+}$-NDPase is more distantly related to the apyrases characterized in *C. lectularius* and *P. papatasii* (37 and 31%, respectively) and to sequences obtained from *Drosophila melanogaster* and *Anopheles gambiae*. Multiple sequence alignment of 10 sequences detected by similarity searches depicts two major groups. One group is formed by the insect sequences. Two of these have been characterized and identified as apyrases. The second group comprises related mammalian sequences, a sequence from the frog *Silurana tropicalis* and one from the nematode *Caenorhabditis elegans*. No related sequence could be detected in yeast (*Saccharomyces cerevisiae*) databases.

The alignment of 10 selected sequences from vertebrate and invertebrate sources reveals several conserved clusters of amino acid residues (Fig. 2). We identified eight motifs that are particularly highly conserved, one of which is directly located at the carboxyl terminus. These include amino acid positions (rat sequence) 107–116, 164–192, 199–232, 281–291, 297–305, 315–323, 345–367, 396–402. The alignment further reveals that all vertebrate sequences contain an extended amino terminus and share the three in-frame start codons. The sequence of *C. elegans* begins with a methionine corresponding to the third start codon of the mammalian sequences. *Drosophila* contains the longest sequence, with three start codons in-frame unrelated to the mammalian sequences. Although all vertebrate sequences share the two hydrophobic stretches at the amino terminus, the invertebrate sequences have only one predicted hydrophobic stretch at the amino terminus. The shortest sequences are those of the bloodsucking insects (*C. lectularius* and the two sandflies, *Lutzomia longipalpis* and *P. papatasi*). No identities were observed with other nucleotide binding or hydrolyzing enzymes.

*Northern Blot Analysis*—To analyze the tissue distribution of the $Ca^{2+}$-NDPase, polyadenylated RNA was purified from rat tissues and probed with a 726-bp antisense probe. Signals were obtained for all tissues analyzed, including intestine, thymus, heart, lung, spleen, kidney, liver, testis, skeletal muscle, and brain (Fig. 3). Two major bands, whose preponderance considerably varied between tissues, were detected at 2.9 and 4.9 kb. Although in several tissues the 4.9-kb form predominated, the 2.9-kb signal was strong in lung, kidney, and brain. The 2.9-kb signal was absent from testis. An mRNA sequence of similar size (3.3 kb) was translated from a human cDNA library (BC017655).

*Expression and Biochemical Characterization*—Transfection of CHO cells with either Myc-tagged full-length or truncated $Ca^{2+}$-NDPase cDNA revealed that both cDNAs are expressed. Cells transfected with the empty plasmid served as a control. Membrane fractions were subjected to Western blot analysis (Fig. 4). After transfection with the full-length clone, a strong immunoreactive band of 49.3 kDa and a weak immunoreactive

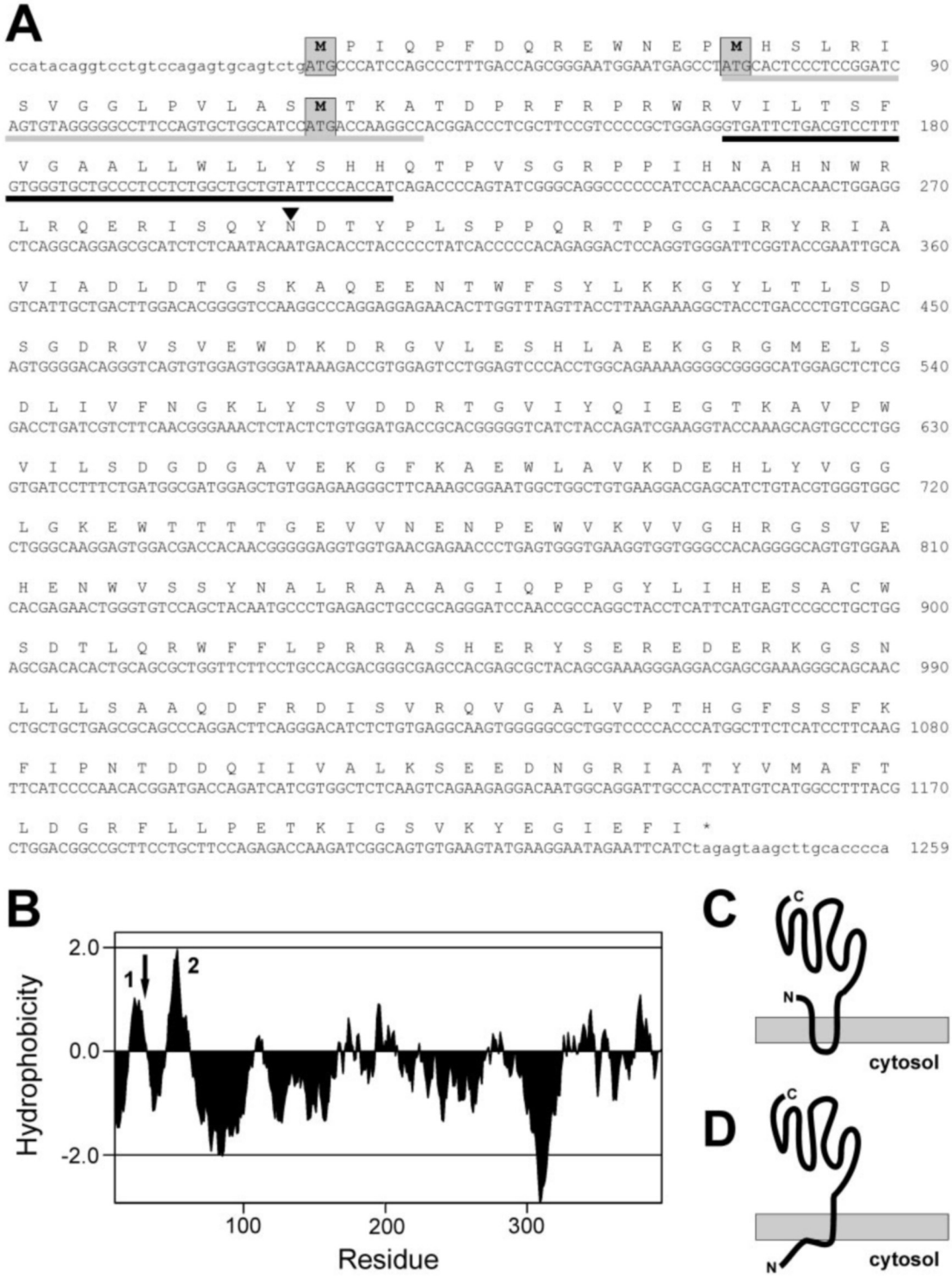


FIG. 1. **DNA sequence, predicted protein sequence, and hydrophobicity plot of rat $Ca^{2+}$-NDPase.** *A*, the three start codons in-frame are indicated by *shading*. Predicted weak and strong hydrophobic sequences are indicated by *gray* and *black bars*, respectively. The *arrowhead* depicts the position of the potential *N*-glycosylation site. *B*, the hydrophobicity plot was prepared by the method of Kyte and Doolittle (21) (window size: 11 residues). The two predicted transmembrane domains are labeled *peak 1*, weak TM, and *peak 2*, strong TM. The *arrow* marks the position of the third start codon utilized in the truncated cDNA. *C* and *D* depict the membrane topography of the full-length $Ca^{2+}$-NDPase.

band of 46.8 kDa were obtained. The molecular mass of the truncated form (46.8 kDa) was identical to that of the weak band obtained after transfection with full-length cDNA. Because the predicted molecular mass of the tagged recombinant full-length protein is 49.6 kDa (untagged 45.7 KDa) and that of the tagged truncated form 46.2 kDa (untagged 42.3 KDa), it is likely that the third start codon is used to a minor extent for protein translation. No immunoreactive bands were obtained when the culture medium or the supernatant fractions obtained after homogenizing transfected cells were analyzed (data not shown). This suggests that no soluble and released form of the protein was generated.

Catalytic activities were determined using membrane fractions obtained from CHO cells transfected with the untagged full-length or truncated cDNA or the empty plasmid (control). Transfection with either cDNA resulted in the formation of

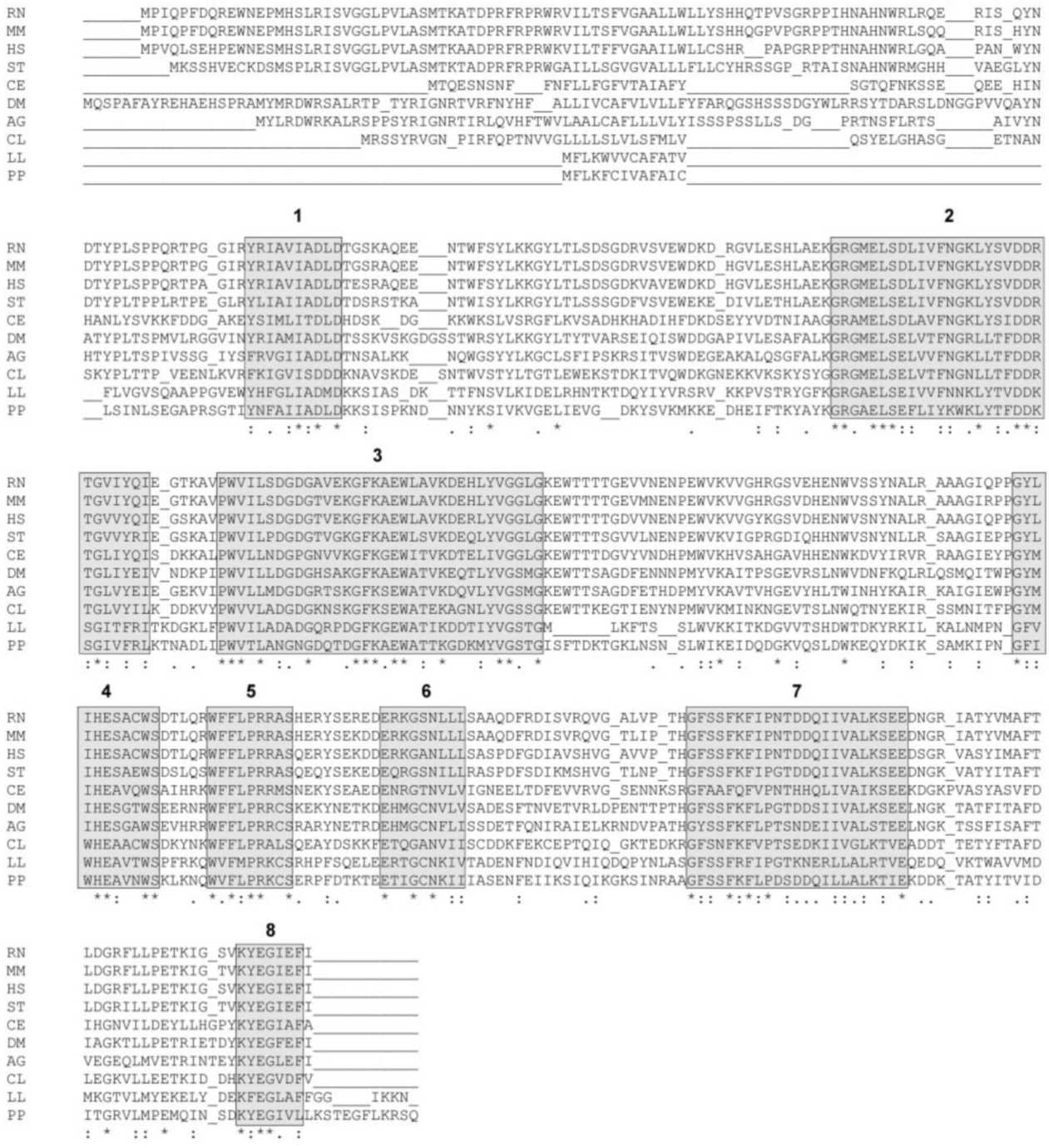


FIG. 2. **Alignment of selected sequences.** Sequence alignment was performed using the CLUSTAL W algorithm. The GenBank™ accession numbers of the sequences are given in parentheses. RN, *Rattus norvegicus* (AJ312207); MM, *Mus musculus* (BC020003); HS, *Homo sapiens* (NT010664); ST, *S. tropicalis* (AL594966, AL645454, AL629683, AL639153, and AL630505, EST consensus sequence); CE, *C. elegans* (U29378, theoretical gene product); DM, *D. melanogaster* (AAF54638, theoretical gene product); AG, *A. gambiae* (AJ297933, frameshift error corrected); CL, *C. lectularius* (AF085499); LL, *L. longipalpis* (AF131933); PP, *P. papatasi* (AF261768). Eight highly conserved sequence domains are indicated by *shading*. (*), single, fully conserved residues. (:), strong group, fully conserved residues. (.), weaker group, fully conserved residues.

catalytically active enzymes with essentially identical substrate specificities and extents of product formation (Fig. 5). Both enzymes revealed highest activities with UDP, GDP, and IDP as substrates. Catalytic activity was very low with CDP as a substrate and absent with ADP. Nucleoside triphosphates were hydrolyzed to a small extent, with the highest catalytic activity obtained with UTP and GTP. Because commercially available nucleoside triphosphates can contain significant amounts of nucleoside diphosphates (8, 10) it is possible that nucleoside diphosphates contributed to the apparent nucleoside triphosphatase activities determined. No hydrolysis was obtained with the corresponding nucleoside monophosphates.

Dependence on divalent metal cations was determined using the full-length protein and UDP, the substrate yielding the highest catalytic activity (Fig. 6). Catalytic activity revealed a strict dependence on $Ca^{2+}$. It was not activated by $Mg^{2+}$ (Fig. 6*A*). At a UDP concentration of 0.5 mM, maximum activity was obtained with 1 mM $Ca^{2+}$. Higher $Ca^{2+}$ concentrations reduced catalytic activity. In the absence of added divalent cations and in the presence of 1 mM EDTA, catalytic activity amounted to 2.8% of maximal activity. Catalytic activity was maximal between pH 6.5 and 7.5 (0.5 mM UDP, 1 mM $Ca^{2+}$) (Fig. 6*B*). The

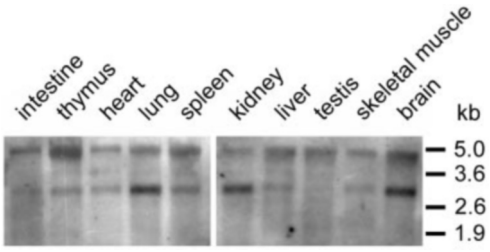


FIG. 3. **Northern blot analysis of $Ca^{2+}$-NDPase mRNA expression in various rat tissues.** Polyadenylated RNA (0.75 $\mu$g per lane) isolated from adult rat tissues was hybridized with a 726-bp digoxigenin-labeled riboprobe.

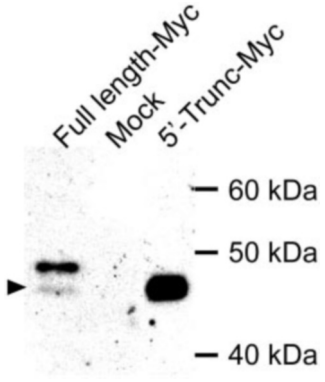


FIG. 4. **Western blots of full-length Myc His-tagged $Ca^{2+}$-NDPase and of the corresponding tagged 5′-truncated protein.** Membrane fractions were prepared from transfected CHO cells, and 3.5 $\mu$g of protein was loaded per lane. In the case of the 5′-truncated protein the third start-codon in-frame was used. The *arrowhead* marks a weak protein band at 46.8 kDa corresponding to the truncated protein.

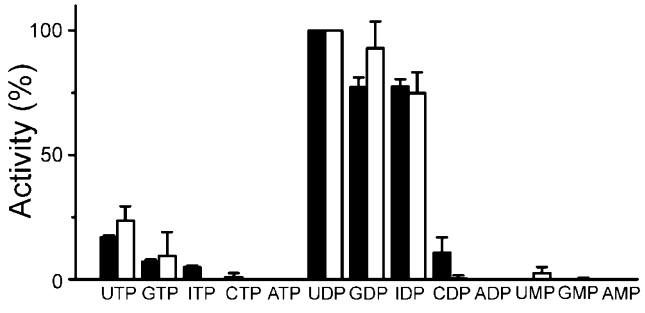


FIG. 5. **Substrate specificity of $Ca^{2+}$-NDPase after heterologous expression in CHO cells.** Membrane fractions were obtained from cells transfected with the untagged full-length (*black bars*) or truncated (*white bars*) cDNA. Substrates were applied at a concentration of 0.5 mM in the presence of 1 mM $CaCl_2$. Catalytic activities were normalized to UDPase activity. The 100% value corresponds to 73 ± 3 nmol $P_i$/($10^6$ cells × min) (± S.E.; $n$ = 3) for the full-length enzyme and 65 ± 38 nmol $P_i$/($10^6$ cells × min) (± S.E.; $n$ = 3) for the 5′-truncated enzyme.

$K_m$ value for UDP at pH 7 was 216 ± 14 $\mu$M (mean ± S.E., $n$ = 3) (Fig. 6*C*).

To further address the solubility of the expressed enzymes, membrane fractions derived from cells transfected with either the full-length cDNA, the truncated cDNA, or the empty plasmid were subjected to Triton X-114 partitioning. Of the specific activity recovered (30–35%), 1.0 and 99.0% were contained in the aqueous and hydrophobic phase, respectively, for the full-length enzyme and 5.6 and 94.4%, respectively, for the truncated enzyme (means of two experiments). This suggests that both forms of the enzyme are membrane-bound.

To investigate whether catalytic activity was in membrane-occluded form or facing the surface of the vesicular organelles generated by cell homogenization in isotonic medium, we compared the catalytic activity before and after addition of Triton X-100 (0.02%) and after treatment with proteinase K. At the critical micellar concentration, Triton X-100 caused no reduction in nucleotidase activity. Membrane fractions derived from mock-transfected cells were compared with those derived from cells transfected with the full-length $Ca^{2+}$-NDPase cDNA. Application of Triton X-100 alone increased 4-fold UDPase activity of membranes from cells transfected with $Ca^{2+}$-NDPase (Fig. 7, *A* and *B*). This catalytic activity was 9.6-fold higher than that obtained under identical conditions with membrane fractions derived from mock-transfected cells (Fig. 7*B*). Addition of proteinase K in the absence of Triton X-100 essentially eliminated catalytic activity (Fig. 7, *A* and *C*). In additional experiments membrane proteins were digested with proteinase K, followed by inactivation of the enzyme with phenylmethylsulfonyl fluoride. Membranes were then treated with Triton X-100 and assayed for $Ca^{2+}$-NDPase activity. This resulted in an 42-fold increase in catalytic activity of membranes containing the recombinant enzyme (Fig. 7, *C* and *D*), suggesting the presence of an occluded and lumenal pool of the enzyme. Accordingly, catalytic activity was strongly reduced when proteinase K and Triton X-100 were co-applied (Fig. 7*E*). Membrane fractions derived from mock-transfected cells contained an endogenous lumenal pool of UDPase activity. Catalytic activity

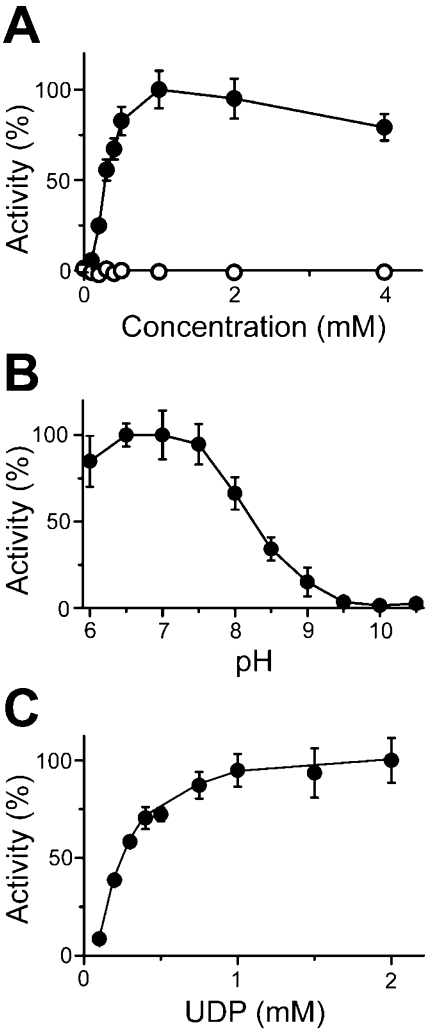


FIG. 6. **Catalytic properties of rat full-length $Ca^{2+}$-NDPase.** *A*, determination of metal cation dependence revealed a strong activation by $Ca^{2+}$ (*filled circles*) but not by $Mg^{2+}$ (*empty circles*). *B*, pH dependence of catalytic rate. *C*, concentration dependence of catalytic rate. Values are means ± S.E.; $n$ = 3.

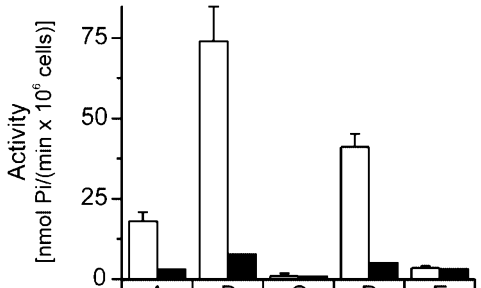


| | | A | B | C | D | E |
|---|---|---|---|---|---|---|
| Preincubation | Proteinase K | - | - | + | + | + |
| | Triton X-100 | - | + | - | - | + |
| Activity assay | Triton X-100 | - | + | - | + | + |

FIG. 7. **Lumenal orientation of $Ca^{2+}$-NDPase as revealed by proteinase K digestion.** Membrane fractions prepared in isotonic buffer were obtained from cells transfected with cDNA encoding untagged full-length $Ca^{2+}$-NDPase (*white bars*) or with the empty plasmid (*black bars*). Membrane fractions were preincubated either in the absence or presence of proteinase K (2.5 $\mu$g) and Triton X-100 (0.02%) as indicated. Either Triton X-100 was added together with proteinase K or membrane fractions were first treated with proteinase K, followed by inactivation of the enzyme with phenylmethylsulfonyl fluoride and addition of Triton X-100. Values are means ± S.E.; $n = 3$.

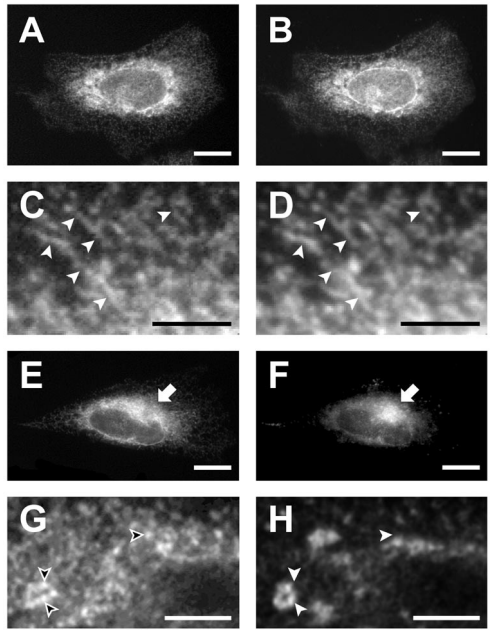


FIG. 8. **Immunocytochemical detection of full-length $Ca^{2+}$-NDPase after transfection into CHO cells.** *A* and *B*, double labeling for $Ca^{2+}$-NDPase (anti-Myc antibody, fluorescein isothiocyanate immunofluorescence, *panel A*) and calnexin (indirect CY3 immunofluorescence, *panel B*). *C* and *D*, high resolution image revealing details of an intracellular reticular network following double labeling for $Ca^{2+}$-NDPase (*C*) and calnexin (*D*) as for *A* and *B*. A few examples of colocalization are indicated by *arrowheads*. *E* and *F*, double labeling for $Ca^{2+}$-NDPase (anti-Myc antibody, CY3 immunofluorescence, *panel E*) and WGA (AlexaFluor-488™-labeled, *panel F*). The *arrow* indicates a focus of strong WGA labeling that is not matched by immunolabeling for $Ca^{2+}$-NDPase. *G* and *H*, high resolution confocal image revealing a close apposition of structures double labeled for $Ca^{2+}$-NDPase (*G*) and WGA (*H*), as for *E* and *F*. The *arrowheads* in *G* and *H* indicate identical positions within the two images. *Bar* indicates 10 $\mu$m, *A*, *B*, *E*, *F* and 3 $\mu$m, *C*, *D*, *G*, *H*.

was enhanced by a factor of 2.5 following treatment with Triton X-100 (Fig. 7, *A* and *B*). Furthermore, occluded endogenous UDPase activity could be demonstrated by treatment with proteinase K (Fig. 7, *C* and *D*).

*Cellular Localization*—Tagged $Ca^{2+}$-NDPase was localized in transfected CHO cells by immunocytochemistry using a monoclonal antibody against the Myc epitope (Fig. 8). When the antibody was applied to CHO cells fixed with methanol 2 d after transfection, the protein could be detected within an intracellular reticular network. To identify the immunolableled cellular compartment, cells were double labeled with an antibody directed against calnexin, a chaperone localized in the ER (26). As shown in Fig. 8, *A–D*, there is a high degree of colocalization for the full-length protein, suggesting that $Ca^{2+}$-NDPase is targeted to the ER. Double labeling with WGA, which exhibits strong binding to the medial and trans cisternae of the Golgi apparatus (27), shows that the $Ca^{2+}$-NDPase reveals a cellular distribution different from the majority of the Golgi compartment (Fig. 8, *E* and *F*). However, when analyzed at high resolution, organellar compartments with increased $Ca^{2+}$-NDPase immunoreactivity were observed in close proximity to individual Golgi stacks (Fig. 8, *G* and *H*). Superimposed images revealed that there is not direct colocalization. Identical results were obtained with the truncated form of the protein (data not shown). No immunolabeling could be obtained when primary antibodies were applied to the surface of viable cells transfected with either the full-length or the truncated cDNA (data not shown).

## DISCUSSION

Here we describe a novel nucleoside diphosphatase of broad tissue distribution capable of hydrolyzing UDP, GDP, and IDP. It is activated by $Ca^{2+}$ but not by $Mg^{2+}$, with a maximal hydrolysis rate between pH 6.5 and 7.5. The amino-terminal sequence contains three putative start codons, two of which appear to be used, resulting in the full-length form and traces of a truncated form of the enzyme. Transfection with a truncated cDNA beginning with the putative third start codon yielded a truncated protein of functional properties and cellular localization identical to the full-length protein. This suggests that the targeting information is located after the third methionine. The large carboxyl-terminal domain with the catalytic site faces the organelle lumen.

$Ca^{2+}$-NDPase displays between 30 and 40% sequence identity with the *C. lectularius* and *P. papatasi* apyrases (19, 20). It shares strict $Ca^{2+}$ dependence and a single potential *N*-glycosylation site with the two *Cimex*-type apyrases. Because of an extended amino terminus, both its calculated and apparent molecular mass is larger (~46 kDa) than those of the *Cimex* type apyrases (~36 kDa). A comparable amino-terminal extension is also observed in the related vertebrate sequences. In all vertebrate species, the amino terminus contains the basic R*X*R ER retention/retrieval motif situated before the putative transmembrane domain. This motif has been ascribed to a number of membrane proteins such as ligand-gated ion channels, G-protein-coupled receptors, or potassium channels. Masking of the R*X*R retention/retrieval motif is thought to play an important role in regulating the forward trafficking of ion channels and other membrane proteins through the secretory pathway (25). This motif may be responsible for the retention of the $Ca^{2+}$-NDPase within the ER.

Sequence shortening and signal peptide cleavage may be a specific adaptive feature of the bloodsucking insects. The predicted reading frame in *D. melanogaster* (44% sequence identity with $Ca^{2+}$-NDPase) is even longer than that of the mammalian sequences. Function and cellular localization of the resulting *Drosophila* protein remain to be determined. Multiple sequence alignment places the insect sequences into a group separate from the vertebrate sequences. Interestingly, the *C. elegans* sequence is grouped into the latter, further supporting the notion of a separate development of the insect genes. The sequence of $Ca^{2+}$-NDPase does not contain consensus sequences identified in nucleotide binding proteins (28). The dis-

tribution over the entire reading frame of sequence domains highly conserved between *C. elegans* and mammals suggests that these may cooperate in nucleotide binding and hydrolysis within the folded protein, similar to the apyrase conserved regions of the E-NTPDase family (29) and to conserved sequence domains in the ecto-5′-nucleotidase family (30, 31).

Functionally, $Ca^{2+}$-NDPase is much more closely related to intracellularly located members of the E-NTPDase family. Its catalytic properties most resemble those of the two $Ca^{2+}$- or $Mg^{2+}$-activated nucleoside diphosphatases, NTPDase5 and NTPDase6. NTPDase5 (CD39L4, ER UDPase) isolated from murine liver revealed a substrate preference of UDP >GDP, IDP >>>ADP, CDP (8), similar to the heterologously expressed human enzyme (UDP >GDP >CDP >ADP) (9). Apparently, NTPDase5 resides in the ER and can be released from cells. The soluble protein has a molecular mass of 45 kDa and a $K_m$ value for UDP of 0.2–0.5 mM (8), similar to $Ca^{2+}$-NDPase (216 $\mu$M). Rat NTPDase6 reveals a strong substrate preference for nucleoside diphosphates (GDP >IDP ≫UDP, CDP ≫ADP) but is expressed to the Golgi apparatus and partially to the cell surface and is released from cells (10). The additional Golgi-localized nucleotidase NTPDase4 (UDPase/hLALPP70v) differs from the other enzymes by hydrolyzing a variety of nucleoside triphosphates in addition to UDP and GDP and by its preference for $Ca^{2+}$ >$Mg^{2+}$ in activating catalytic activity (5, 7). The exact subcellular localization of NTPDase7 (LALP1) with its preferred substrates UTP, GTP, and CTP is still undefined (14). Its catalytic properties resemble those of the lysosome/autophagic vacuole-located variant of NTPDase4 (hALAP70) (UTP >TTP >CDP >UDP = CTP) (7).

A major question is the functional role of the enzymes targeted to ER and Golgi apparatus. Yeast contains two Golgi-located enzymes related to NTPDase4 (Ynd1/Apy1p, Refs. 16 and 17) and NTPDase5/6 (yeast GDPase, Ref. 15) but no sequence related to the $Ca^{2+}$-NDPase. Double deletion experiments revealed that the two yeast enzymes are required for Golgi glycosylation and cell wall integrity (16). Rat NTPDase5 (ER-UDPase) has been suggested to promote reglycosylation reactions involved in glycoprotein folding and quality control in the ER (8). According to this model, misfolded proteins are recognized by soluble UDP-glucose:glycoprotein glycosyltransferase that adds a single glucose residue back to the trimmed oligosaccharide, resulting in a second round of folding by a chaperone (26, 32). UDP-glucose required for the glycosylation reaction is taken up into the ER via a nucleotide sugar/nucleoside monophosphate antiporter (33, 34). The resulting UDP is cleaved to UMP by lumenal nucleoside diphosphatase, and the nucleoside monophosphates formed are then exchanged via the antiporter system for more nucleotide sugar. An additional possibility would be that UDP-hydrolyzing enzymes could be involved in the utilization of UDP derived from UDP-*N*-acetylglucosamine and UDP-glucuronic acid that are also imported from the cytosol into the ER lumen (8, 33).

Our results suggest that the ER contains a membrane-bound enzyme with the capability to hydrolyze UDP, GDP, and IDP, in addition to the soluble NTPDase5 (ER-UDPase, CD39L4). Although mammalian cells transport CMP-, GDP-,and UDP-sugars into the Golgi apparatus, only UDP-sugars are known to be imported into the ER (33). At present the catalytic potential for the hydrolysis of GDP and IDP within the ER remains enigmatic. It also needs to be investigated whether the two ER nucleoside diphosphatases are equally distributed throughout the entire ER. Following heterologous transfection, $Ca^{2+}$-NDPase is targeted to the ER, but the increased immunolabeling at sites close to WGA-labeled Golgi stacks implies that the enzyme may also enter membrane compartments intermediate between the ER and Golgi apparatus (35). Interestingly, the ER protein-folding sensor UDP-glucose:glycoprotein glycosyltransferase is enriched in pre-Golgi intermediates, suggesting that this compartment may participate in protein quality control (36). Because quality control represents an essential step in the secretory assembly line (26), expression of two different proteins with overlapping catalytic activities may represent a safety margin. It is also possible that the preponderance of the two enzymes varies between cell types and tissues. This notion is supported by a comparison of our Northern blot analyses with those obtained for human NTPDase5 (CD39L4) (37).

ATP is actively transported into the ER and Golgi apparatus (38, 39). Within the ER it serves a variety of energy-requiring reactions, including protein translocation, dissociation of complexes among chaperones and correctly folded and assembled proteins, disulfide bond formation, and lumenal phosphorylation of proteins (33, 40). It is therefore not surprising that nucleotidases resident both in the ER and Golgi apparatus lack significant ATPase activity. However, all nucleotidases, including those hydrolyzing ATP and destined to the cell surface, need to pass through the ER. This raises the question whether they are prevented from hydrolyzing nucleotides within the secretory pathway. It has been shown for the ATP- and ADP-hydrolyzing ecto-nucleotidase, NTPDase1, that as a result of incomplete glycosylation the enzyme remains inactive intracellularly (41). Our investigation adds another nucleotidase to the mammalian cellular endomembrane system. The multiplicity of nucleoside tri- and/or diphosphate-hydrolyzing enzymes within the various compartments of the endomembrane system, including ER (8, 9), Golgi apparatus (5, 10), lysosomes, autophagic vacuoles (6, 7), and (presumably) additional organellar structures (14) implies the presence of the substrate nucleotides in the respective compartments. This provides a challenge for a more detailed investigation of nucleotide function and metabolism within the endomembrane system.

*Acknowledgment*—We thank Peter Brendel for expert technical support.

REFERENCES

1. Zimmermann, H. (2001) in *Handbook of Experimental Pharmacology. Purinergic and Pyrimidergic Signalling I* (Abbracchio, M. P., and Williams, M., eds), pp. 209–250, Springer Verlag, Heidelberg
2. Zimmermann, H. (2001) *Drug Dev. Res.* **52,** 44–56
3. Enjyoji, K., Sévigny, J., Lin, Y., Frenette, P., Christie, P. D., Schulte am Esch, J., Imai, M., Edelberger, J. M., Rayburn, H., Lech, M., Beeler, D. M., Csizmadia, E., Wagner, D. D., Robson, S. C., and Rosenberg, R. D. (1999) *Nat. Med.* **5,** 1010–1017
4. Dunwiddie, T. V., Diao, L. H., and Proctor, W. R. (1997) *J. Neurosci.* **17,** 7673–7682
5. Wang, T. F., and Guidotti, G. (1998) *J. Biol. Chem.* **273,** 11392–11399
6. Biederbick, A., Rose, S., and Elsässer, H. P. (1999) *J. Cell Sci.* **112,** 2473–2484
7. Biederbick, A., Kosan, C., Kunz, J., and Elsässer, H. P. (2000) *J. Biol. Chem.* **275,** 19018–19024
8. Trombetta, E. S., and Helenius, A. (1999) *EMBO J.* **18,** 3282–3292
9. Mulero, J. J., Yeung, G., Nelken, S. T., and Ford, J. E. (1999) *J. Biol. Chem.* **29,** 20064–20067
10. Braun, N., Fengler, S., Ebeling, C., Servos, J., and Zimmermann, H. (2000) *Biochem. J.* **351,** 639–647
11. Hicks-Berger, C. A., Chadwick, B. P., Frischauf, A. M., and Kirley, T. L. (2000) *J. Biol. Chem.* **275,** 34041–34045
12. Mulero, J. J., Yeung, G., Nelken, S. T., Bright, J. M., McGowan, D. W., and Ford, J. E. (2000) *Biochemistry* **39,** 12924–12928
13. Yeung, G., Mulero, J. J., McGowan, D. W., Bajwa, S. S., and Ford, J. E. (2000) *Biochemistry* **39,** 12916–12923
14. Shi, J. D., Kukar, T., Wang, C. Y., Li, Q. Z., Cruz, P. E., Davoodi-Semiromi, A., Yang, P., Gu, Y. R., Lian, W., Wu, D. H., and She, J. X. (2001) *J. Biol. Chem.* **276,** 17474–17478
15. Abeijon, C., Yanagisawa, K., Mandon, E. C., Häusler, A., Moremen, K., Hirschberg, C. B., and Robbins, P. W. (1993) *J. Cell Biol.* **122,** 307–323
16. Gao, X. D., Kaigorodov, V., and Jigami, Y. (1999) *J. Biol. Chem.* **274,** 21450–21456
17. Zhong, X. T., and Guidotti, G. (1999) *J. Biol. Chem.* **274,** 32704–32711
18. Lopez-Avalos, M. D., Uccelletti, D., Abeijon, C., and Hirschberg, C. B. (2001) *Glycobiology* **11,** 413–422
19. Valenzuela, J. G., Charlab, R., Galperin, M. Y., and Ribeiro, J. M. C. (1998) *J. Biol. Chem.* **273,** 30583–30590
20. Valenzuela, J. G., Belkaid, Y., Rowton, E., and Ribeiro, J. M. C. (2001) *J. Exp. Biol.* **204,** 229–237

21. Kyte, J., and Doolittle, R. F. (1982) *J. Mol. Biol.* **157,** 105–132
22. Kegel, B., Braun, N., Heine, P., Maliszewski, C. R., and Zimmermann, H. (1997) *Neuropharmacology* **36,** 1189–1200
23. Lanzetta, P. A., Alvarez, L. J., Reinach, P. S., and Candia, O. A. (1979) *Anal. Biochem.* **100,** 95–97
24. Heilbronn, A., Krapohl, A., and Zimmermann, H. (1995) *Cell Tissue Res.* **280,** 123–131
25. Scott, D. B., Blanpied, T. A., Swanson, G. T., Zhang, C., and Ehlers, M. D. (2001) *J. Neurosci.* **21,** 3063–3072
26. Helenius, A. (2001) *Philos. Trans. R. Soc. Lond.-Biol. Sci.* **356,** 147–150
27. Parkkinen, J. J., Lammi, M. J., Agren, U., Tammi, M., Keinanen, T. A., Hyvonen, T., and Eloranta, T. O. (1997) *J. Cell. Biochem.* **66,** 165–174
28. Saraste, M., Sibbald, P. R., and Wittinghofer, A. (1990) *Trends Biochem. Sci.* **15,** 430–434
29. Yang, F., Hicks-Berger, C. A., Smith, T. M., and Kirley, T. L. (2001) *Biochemistry* **40,** 3943–3950
30. Zimmermann, H. (1992) *Biochem. J.* **285,** 345–365
31. Knöfel, T., and Sträter, N. (1999) *Nat. Struct. Biol.* **6,** 448–453
32. Ellgaard, L., Molinari, M., and Helenius, A. (1999) *Science* **286,** 1882–1888
33. Hirschberg, C. B., Robbins, P. W., and Abeijon, C. (1998) *Annu. Rev. Biochem.* **67,** 49–69
34. Castro, O., Chen, L. Y., Parodi, A. J., and Abeijón, C. (1999) *Mol. Biol. Cell* **10,** 1019–1030
35. Gomord, V., Wee, E., and Faye, L. (1999) *Biochimie (Paris)* **81,** 607–618
36. Zuber, C., Fan, J.-Y., Guhl, B., Parodi, A., Fessler, J. H., Parker, C., and Roth, J. (2001) *Proc. Natl. Acad. Sci. U. S. A.* **98,** 10710–10715
37. Chadwick, B. P., and Frischauf, A. M. (1998) *Genomics* **50,** 357–367
38. Guillen, E., and Hirschberg, C. B. (1995) *Biochemistry* **34,** 5472–5476
39. Puglielli, L., Mandon, E. C., and Hirschberg, C. B. (1999) *J. Biol. Chem.* **274,** 12665–12669
40. Bukau, B., and Horwich, A. L. (1998) *Cell* **92,** 351–366
41. Zhong, X. T., Malhotra, R., Woodruff, R., and Guidotti, G. (2001) *J. Biol. Chem.* **276,** 41518–41525